

1 **Effect of synchronization of firings of different motor unit types on the force variability**
2 **in a model of the rat medial gastrocnemius muscle**

3 Rositsa Raikova ^{*2}, Vessela Krasteva ², Piotr Krutki¹, Hanna Drzymała-Celichowska ¹,
4 Katarzyna Kryściak ¹, and Jan Celichowski ¹

5

6 ¹ Department of Neurobiology, Poznan University of Physical Education, Poznan, Poland

7 ² Institute of Biophysics and Biomedical Engineering, Bulgarian Academy of Sciences, Sofia,
8 Bulgaria

9 * Corresponding author: rosi.raikova@biomed.bas.bg

10

11 Short title:

12 **Synchronization of motor units in a model of the rat medial gastrocnemius muscle**

14 **Abstract**

15 Oscillations of muscle force, observed as physiological tremors, rely upon the synchronized
16 firings of active motor units (MUs). This study aimed to investigate the effects of
17 synchronizing the firings of three types of MUs on force development using a mathematical
18 model of the rat medial gastrocnemius muscle. The model was designed based on the actual
19 proportion and physiological properties of MUs and motoneurons innervating the muscle.
20 The isometric muscle and MU forces were simulated by a model predicting non-synchronized
21 firing of a pool of 57 MUs (including eight slow, 23 fast resistant to fatigue, and 26 fast
22 fatigable) to ascertain a maximum excitatory signal when all MUs were recruited into the
23 contraction. The mean firing frequency of each MU depended upon the twitch contraction
24 time, whereas the recruitment order was determined according to increasing forces (the size
25 principle). The synchronization of firings of individual MUs was simulated using four
26 different modes and inducing the synchronization of firings within three time windows (± 2 ,
27 ± 4 , and ± 6 ms) for four different combinations of MUs. The synchronization was estimated
28 using two parameters, the correlation coefficient and the cross-interval synchronization index.
29 The four scenarios of synchronization increased the values of the root-mean-square, range,
30 and maximum force in correlation with the increase of the time window. Greater
31 synchronization index values resulted in higher root-mean-square, range, and maximum of
32 force outcomes for all MU types as well as for the whole muscle output; however, the mean
33 spectral frequency of the forces decreased, whereas the mean force remained nearly
34 unchanged. The range of variability and the root-mean-square of forces were higher for fast
35 MUs than for slow MUs; meanwhile, the relative values of these parameters were highest for
36 slow MUs, indicating their important contribution to muscle tremor, especially during weak
37 contractions.

38 **Keywords:** muscle, motor unit, synchronization, medial gastrocnemius, muscle force

39

41 **Author summary**

42 The synchronization of firings of motor units (MUs), the smallest functional elements of
43 skeletal muscle increases fluctuations in muscle force, known as physiological tremor, which
44 can disturb high-precision movements. In this study, we adopted a recently proposed muscle
45 model consisting of MUs of three different types (fast fatigable, fast resistant to fatigue, and
46 slow) to study four different scenarios of MU synchronization during a steady level of
47 excitatory input to motoneurons. The discharge patterns were synchronized between pairs of
48 MUs by shifting in time individual pulses, which occurred within a short time interval, and a
49 degree of synchronization was then estimated. The increased synchronization index resulted
50 in increased force variability for all MU types as well as for the whole muscle output;
51 however, the mean force levels remained nearly unchanged, whereas the frequencies of the
52 force oscillations were decreased. The absolute range of force variability was higher for fast
53 than for slow MUs, indicating their dominant influence on muscle tremor at strong
54 contractions, but the highest relative increase in force variability was observed for
55 synchronized slow MUs, indicating their significant contribution to tremor during weak
56 contractions, in which only slow MUs are active.

57 **Introduction**

58 Most studies of motor unit (MU) firings have revealed the existence of a certain level of
59 synchronization between the firings of motoneurons innervating the same muscle [1-4]. Two
60 concepts for long- and short-term synchronization can be found in the literature. Long-term
61 synchronization with greater latencies beyond ± 20 ms was reported by Datta and Stephens,
62 De Luca et al., Kirkwood et al., Schmied et al., and Semmler et al. [1, 4–7]. The possible
63 mechanism of this kind of synchronization could be explained as interactions occurring
64 between the stretch reflex loop and the recurrent inhibition. Long-term synchronization has
65 been reported to be relatively rare relative to short-term synchronization [4], which was
66 reported to be a peak in the cross-interval histogram centered about a zero-time delay ($0.5 \pm$
67 2.9 ms). Short-term synchronization is attributed to last-order projections that provide
68 common, nearly simultaneous, excitatory synaptic input across motoneurons [3, 8, 9],
69 generating a narrow peak around the origin of the cross-correlogram of MU discharges [1, 8,
70 10, 11]. Therefore, the narrow synchronous peak principally reflects shared, monosynaptic
71 projections to motor neurons from corticomotoneuronal cells via the lateral corticospinal tract
72 [12].

73 In humans, the MU synchronization was shown to be stronger during voluntary
74 muscle activation than during reflex activation [13]. At the same time, synchronization tends
75 to be higher in more distally located muscles, while the greatest synchrony has been most
76 often found in the intrinsic muscles of the foot rather than in the hand muscles [3, 14].
77 However, the level of synchronization between MUs could be influenced by numerous
78 factors, such as the examined task, the muscles involved in the task, and the type of habitual
79 physical activity performed by the individual [6-7, 15-18]. For example, the level of
80 synchronization was reduced between MUs in the hand muscles of individuals who required

81 greater independent control of the fingers. This included musicians [17] and the dominant
82 hands of control subjects [7]. On the other hand, MU synchronization was found to be greater
83 in the hand muscles of individuals who consistently performed strength training [17, 19] or
84 during tasks that demanded attention [20]. The enhancement of MU synchronization was
85 observed after daily exercise involving brief periods of maximal muscular contraction [19]
86 and contributed to training-induced increments in muscle strength [21]. Better
87 synchronization has also been noted in fatigued muscles [22]. Reports regarding the
88 relationship between physiological tremor and synchronization are inconsistent: most of them
89 have linked tremor with an increased level of synchronization [22-25], while others have
90 suggested no significant associations between the tremor amplitude and the level of MU
91 synchronization exist [17].

92 It has been assumed that muscle can produce smooth contractions due to
93 asynchronous discharges of motor neurons [23]. Yao et al. [21] revealed that MU
94 synchronization increased the variability in the simulated force but not the average force.
95 Synchronization was also shown to increase the estimated twitch force of the MUs [26].

96 In the majority of skeletal muscles, three types of MUs have been distinguished and
97 their contractile properties, including the force–frequency of stimulation relationship [27] and
98 sensibility to changes in stimulation pattern [28, 29], were found to vary considerably. In
99 several studies, the effects of the synchronization of MU firings were modelled [21, 30, 31];
100 however, these models did not analyze the specific effects attributable to different types of
101 MUs. In our previous paper [32], a model of the rat medial gastrocnemius muscle consisting
102 of 30 MUs [10 MUs each of the fast fatigable (FF), fast resistant to fatigue (FR), and slow (S)
103 types] was proposed and the effects of synchronous and asynchronous stimulation of MUs
104 were investigated. It was concluded that the activation of MUs at variable interpulse

105 intervals, delivered to each MU asynchronously, resulted in smaller force oscillations.
106 However, the study did not assess the effects of synchronization between pairs of individual
107 MUs nor the effects of the synchronization of three types of MUs.

108 A recent model of the rat medial gastrocnemius muscle [33] provided methodology by
109 which to identify the role of each of three MU types (FF, FR, and S) in the production of
110 muscle force. In the present study, the same model was adopted as a tool for simulation of
111 four modes and three time levels of synchronization. The aim of this research was to reveal
112 the important effects of synchronization on the force variability and the force mean spectral
113 frequency and to compare these effects between all types of MUs and the whole muscle. The
114 implication of the results for explanation of tremor at various levels of the muscle force was
115 discussed.

116

117 **Materials and methods**

118 *Muscle model*

119 This study applied a model of the rat muscle gastrocnemius based on excitability and firing
120 frequencies of motoneurons, contractile properties, and the number and proportion of MUs in
121 the muscle [33]. Briefly, the model consists of 57 MUs, including eight S, 23 FR, and 26 FF
122 MUs, respectively. As input data, this set of MUs, recorded in physiological experiments,
123 was selected and their twitches were precisely modeled by a six-parameter analytical function
124 [34]. The muscle force was calculated as the sum of forces of all active MUs and the process
125 of force regulation was set according to the common-drive hypothesis [35]. The muscle
126 unfused tetanus was calculated following the application of a train of irregular stimuli and

127 was simulated using an analytical approach described in previous research [33, 36].

128 Meanwhile, the scheme of MU firing was adopted from Fuglevand et al. [30].

129 In the present study, the excitation signal is simulated (Fig. 1A) as consisting of two
130 smooth logarithmic parts existing during the increasing and decreasing parts of the muscle
131 force (each lasting 1000 ms) and a straight line present during the steady state of the muscle
132 (lasting 2000 ms). The shape of the signal waveform was designed to better approximate
133 more realistically a course of excitation input to motoneurons, avoiding sudden changes
134 occurring in any trapezoidal signal used previously. This study considered only one
135 excitation level, corresponding to 100% of the activation signal, ensuring that all MUs were
136 activated during the steady state of the muscle to enable a thorough analysis of their
137 synchronization. The program for simulation of the force MUs and the muscle force accepted
138 the same MU firing frequencies as previously described (Table 1 in Raikova et al. [33]). The
139 first MU firings at equal interpulse intervals (IPIs) were calculated and, during a second step,
140 a random shifting of IPIs (within intervals of $0, \pm 1$, and ± 2 ms) was applied, thus simulating
141 a train of firings at irregular IPIs. Finally, the model generated the output forces for different
142 MUs (S, FR, and FF) and the whole muscle, as illustrated in Fig. 1B (sampling frequency $f_s =$
143 1 kHz). This was further denoted as the basic (non-synchronized; *NS*) model, to which no
144 attempts of manual changes of MU firing for synchronization were applied. The force signals
145 were analyzed during the steady-state periods (2000–4000 ms). Their power frequency
146 spectra were calculated by using fast Fourier transform (FFT) over $n_f = 2048$ points, thus
147 achieving a spectral resolution $\Delta f = f_s/n_f = 0.49$ Hz (Figs. 1C–1F). The zero-frequency
148 component defined by the large mean force offset was rejected as soon as it had no relevancy
149 to the frequency components related to the variability of the simulated force, which was
150 under the scope of this study.

151 ***Simulation of MU synchronization***

152 The *NS* firings of all 57 MUs during the muscle steady state are shown in Fig. 2. These
153 patterns were further modified to simulate different types and levels of synchronization. The
154 synchronization was applied to a specific pair of MUs (named MU1 and MU2) so that the
155 impulses of MU2, which fall within a predefined time window, Δt , around the impulses of
156 MU1, were changed to coincide with those of MU1. Three time windows with $\Delta t = \pm 2, \pm 4$
157 or ± 6 ms were used to simulate three levels of MU synchronization, mimicking weak,
158 modest, and strong synchronization, respectively. The synchronization scheme is illustrated
159 in Fig. 3, showing that the larger the time window was, the greater number of more MU
160 pulses were shifted to and synchronized with the reference MU.

161 Four methods of synchronization (Methods 1–4) were applied. In all methods, the
162 synchronized MU pairs were chosen only encompassing the same physiological type (S and
163 S, FR and FR, FF and FF), i.e., synchronization was not induced between MUs of different
164 types.

165 *Method 1*: Two neighboring MUs within the same physiological type according to the
166 recruitment order based on their increasing force of the twitch (see Table 1 in Raikova et al.
167 [33]) were synchronized, i.e., for S MUs, 1–2, 2'–3, ..., 7'–8; for FR MUs, 9–10, 10'–11, ...,
168 30'–31; and, for FF MUs, 32–33, 33'–34, ..., 56'–57. Note that, for each next
169 synchronization, the already synchronized pattern of the previous MU is used and marked by
170 “'” .

171 *Method 2*: Two neighboring MUs within the same physiological type but when ordered
172 according to their increasing mean firing rate (see Table 1 in Raikova et al. [33]), were
173 synchronized i.e., for S MUs, 7-1, 1'–6, 6'–5, 5'–4, 4'–2, 2'–3, and 3'–8; for FR MUs, 18–16,

174 16'–24, 24'–22, 22'–28, 28'–14, 14'–12, 12'–23, 23'–13, 13'–20, 20'–31, 31'–27, 27'–29, 29'–
175 25, 25'–9, 9'–21, 21'–30, 30'–26, 26'–19, 19'–17, 17'–11, 11'–10, and 10'–15; and, for FF
176 MUs, 50–44, 44'–43, 43'–49, 49'–39, 39'–54, 54'–52, 52'–55, 55'–56, 56'–48, 48'–47, 47'–
177 53, 53'–51, 51'–37, 37'–40, 40'–41, 41'–57, 57'–45, 45'–35, 35'–33, 33'–46, 46'–32, 32'–34,
178 34'–38, 38'–36, and 36'–42.

179 *Method 3:* The MUs within the same physiological type but in unique groups of four MUs
180 were synchronized to the first recruited MU and ordered according to their increasing force of
181 the twitch (see Table 1 in Raikova et al. [33]), i.e., for S MUs, 1–2, 1–3, 1–4, 5–6, 5–7, and
182 5–8; for FR MUs: 9–10, 9–11, 9–12, 13–14, 13–15, 13–16, 17–18, 17–19, 17–20, 21–22, 21–
183 23, 21–24, 25–26, 25–27, 25–28, 29–30*, and 29–31*; and, for FF MUs, 32–33, 32–34, 32–
184 35, 36–37, 36–38, 36–39, 40–41, 40–42, 40–43, 44–45, 44–46, 44–47, 48–49, 48–50, 48–51,
185 52–53, 52–54, 52–55, and 56–57*. The symbol (*) denotes the groups, where the number of
186 synchronized MUs was less than four due to the fact that the number of MUs in the
187 respective physiological type was not a multiple of four.

188 *Method 4:* The MUs within the same physiological type were synchronized, taking as a
189 reference the first recruited MU of the specific type (see Table 1 in Raikova et al., [33]), i.e.,
190 for S MUs, 1–2, 1–3, ..., 1–8; for FR MUs, 9–10, 9–11, ..., 9–31; and, for FF MUs, 32–33,
191 32–34, ..., 32–57.

192 ***Estimation of MU synchronization***

193 *Temporal correlation of MU impulses*

194 The MU pulses were represented as an MU binary (MUB) sample series with a
195 constant sampling period of 1 ms and binary amplitude of 0 or 1, where “0” indicated a non-
196 active state and “1” indicated the presence of a pulse-active state. The duration of the pulse-

197 active state was set to 1 ms, overlaying one sampling period. MUB series were represented
198 with a total of 2000 samples during the steady state of the muscle from 2000 ms to 4000 ms,
199 as depicted in Figs. 1 and 2 for the MUs in the basic, *NS* model.

200 The temporal correlation between the binary sample series of two MUs (MUB1 and
201 MUB2) was computed with the normalized Pearson's correlation coefficient ranged in the
202 interval 0% to 100%, according to the following formula:

$$203 \quad corMU = \frac{\sum_{i=2000ms}^{4000ms} MUB1_i \cdot MUB2_i}{\sqrt{\sum_{i=2000ms}^{4000ms} MUB1_i^2 \cdot \sum_{i=2000ms}^{4000ms} MUB2_i^2}} \cdot 100, [\%] \quad (1)$$

204 where i denotes the sample index of the MUB series, considering a sampling period of 1 ms.

205 The correlation coefficient ($corMU$) is a standard measure of similarity between
206 sample series data in the time domain. Transferring this knowledge to the MUB data, $corMU$
207 is representative of the temporal synchronization of two MU firings such that 100%
208 corresponds to a complete coincidence between all firing pulses in MU1 and MU2 and 0%
209 corresponds to no coincidence between any firing pulse in MU1 and MU2. The normalized
210 value of $corMU$ does not depend upon the length of the estimated MUB time series, the
211 number of firing pulses, or the mean firing rate,. This is an important benefit of the
212 normalization, which would prevent bias in $corMU$ estimation, considering that MUs in
213 different physiological types have different mean firing rates.

214 *Cross-interval synchronization index*

215 The synchronization between the firing patterns of two MUs (MU1 and MU2) was estimated
216 by an analysis of their cross-intervals using $CI_x(MU1, MU2) = \{t1_x - t2_{xy}\}$ computed as a
217 pair-wise difference between the times of occurrence of all reference MU1 pulses

218 $t1_x = \{t1_1, t1_2, \dots, t1_{nMU1}\}$ and their corresponding closest neighbors among MU2 pulses
 219 $t2_{xy} \in t2_y = \{t2_1, t2_2, \dots, t2_{nMU2}\}$. The latter were found by the minimization criterion
 220 $t2_{xy} = \arg \min_{y=1,2,\dots,nMU2} \{|t1_x - t2_y|\}$ and respected the condition to overlay only firings during the
 221 steady state of the muscle, i.e., $t1_x, t2_y \in [2000ms; 4000ms]$. By definition, the
 222 $CI_x(MU1, MU2)$ vector length was equal to the number of pulses in the reference MU
 223 ($nMU1$). CI values could be negative, zero, or positive when an MU1 pulse was respectively
 224 preceding, coinciding with or following its neighbor MU2 pulse, as illustrated in Fig. 4.

225 The distribution of cross-interval values of two MUs, $CI(MU1, MU2)$, was estimated
 226 by means of a cross-interval histogram with a bin-width resolution of 1 ms and bin centers in
 227 the range of ± 15 ms. The bin values represented the relative probability (p_{bi}) of having a CI
 228 observation within a specific bin interval (bi):

$$229 \quad p_{bi} = \frac{c_{bi}\{CI(MU1, MU2)\}}{nMU1}, \quad (2)$$

230 accepting the sum of all bin values equal to 1:

$$231 \quad \sum_{bi=-15ms}^{+15ms} p_{bi} = 1 \quad (3)$$

232 where c_{bi} is the count of $CI(MU1, MU2)$ values in bin bi and the denominator is the number
 233 of elements in the input data, equal to the number of reference MU pulses ($nMU1$).

234 Derived from the cross-interval histogram, the synchronization between the firing
 235 patterns of MU1 and MU2 was estimated by the relative probability p_{b0} in the central bin ($b0$
 236 $= \pm 0.5$ ms), equivalent to the relative frequency of coincidence between MU1 and MU2
 237 pulses related to the reference number of pulses:

238
$$p_{b0} = \frac{c_{b0} \{-0.5ms \leq CI(MU1, MU2) < +0.5ms\}}{nMU1} \quad (4)$$

239 Given a total number of $N = 57$ MUs, there could be derived a total of $N-1$ cross-interval
240 vectors $CI(MU_i, MU_j)$ for any given pair of MUs, where $i, j = 1, 2, \dots, N$, and $i \neq j$. Further, a
241 cross-interval synchronization index (*CISI*) was defined for each reference MU_i pattern to
242 accumulate the relative probability of pulse coincidences in all MU_i pairs ($N - 1$) observed in
243 the central bin:

244
$$CISI(MU_i) = \frac{1}{N-1} \sum_{\substack{j=1 \\ j \neq i}}^N \frac{c_0 \{CI(MU_i, MU_j)\}}{nMU_i} \cdot 100, [\%] \quad (5)$$

245 *CISI* has a normalized value from 0 to 100% with 0% corresponding to no coincidence and
246 100% corresponding to a complete coincidence between the patterns of the reference MU_i
247 and all other paired MUs. The adopted *CISI* normalization to both number of MU pairs (N)
248 and number of reference firings (nMU_i) was implemented to reject the influence of the size
249 and type of the studied MU population.

250 *Force parameters*

251 Standard force parameters of the different MU groups (S, FR, and FF) and the cumulative
252 force of the whole muscle (Fig. 1B) were calculated as follows:

- 253 • Force mean value: $meanF = \sum_{i=1}^n \frac{F_i}{n}$
- 254 • Force max value: $max F = max(F_i)$
- 255 • Force min–max range: $rangeF = max(F_i) - min(F_i)$

256 • Force root-mean-square (*RMS*) level: $rmsF = \sqrt{\frac{\sum_{i=1}^n (F_i - meanF)^2}{n}}$

257 where F_i denoted the force signal samples, taken with a sampling period of 1 ms during the
258 steady state of the muscle from 2000 ms to 4000 ms, including a total number of $n = 2000$
259 samples.

260 Additionally, the force power spectral density (*PSD*) of different MU groups (S, FR,
261 and FF) and the cumulative muscle force (Fig. 1C) was used for the calculation of the mean
262 spectral frequency as follows:

$$263 \quad meanfreq = \frac{\sum_{i=1}^{nf} f_i \cdot PSD_i}{\sum_{i=1}^{nf} PSD_i}, [Hz], \quad (6)$$

264 where nf is number of frequency bins in the spectrum ($nf = 2048$ as defined earlier), f_i is the
265 frequency of the spectrum at bin i of nf , and PSD_i is the amplitude of the *PSD* at bin i of nf .

266 **Results**

267 ***Weak synchronization of MU firings in the basic muscle model***

268 The level of synchronization between MU firing patterns of the simulated basic rat muscle
269 gastrocnemius model with 100% excitation containment and 57 MUs, over a two -second time
270 period during the muscle steady state, was estimated by the two different synchronization indices in
271 Table 1 (top row) and discussed as follows.

272 First, $corMU = 6.1\% \pm 2.8\%$ (mean value \pm standard deviation) shows a ***weak***
273 ***temporal*** correlation between the firing pulses of all MUs within the muscle, which was
274 found to be lowest for MUs of type S ($4.5\% \pm 2\%$) and highest for those of type FR ($7.4\% \pm$
275 2.9%). A comprehensive proof for the absence of noteworthy clusters with significant

276 correlation between MUs of a specific type is illustrated in the *corMU* colormap in Fig. 5A.
277 Here, a random distribution of *corMU* values can be noted, overlaying the dark-blue colored
278 area of very low pairwise correlations between 57×57 MUs, distributed on the x- and y-
279 axes. The entries in the main diagonal should be ignored because each represents a MU
280 compared with itself (*corMU* = 100%).

281 Second, $CISI = 6.2\% \pm 0.4\%$ (mean value \pm standard deviation) suggests ***weak*** cross-
282 interval synchronization between the firing pulses of all MUs within the muscle, without
283 essential differences between MUs of different physiological types [the *CISI* mean value
284 varied from 5.8% (S MUs) to 6.2% (FR and FF MUs)]. Evidence for missing synchronization
285 between MU firings can be observed in the cross-interval histograms in Fig. 6A, having a flat
286 (uniform) distribution in the range of bin-intervals $[-6 \text{ ms}; +6 \text{ ms}]$ for all 57 MUs. Therefore,
287 cross-intervals between firing patterns were equally probable within this bin range and no
288 evidence for synchronous peaks could be identified in the case of any MU.

289 ***Stronger synchronization of MU firings in different synchronization scenarios***

290 The aforementioned 57 MU firing patterns of the basic muscle model were modified
291 according to 12 synchronization scenarios, i.e., four synchronization concepts (Methods 1–4)
292 each applied within three synchronization time intervals ($\Delta t = \pm 2, \pm 4, \text{ and } \pm 6 \text{ ms}$). The
293 resultant average levels of synchronization between patterns of MUs of the same
294 physiological type and within the whole muscle are estimated in Table 1. In all cases, certain
295 increments of both indices for the level of MU synchronization (*corMU* and *CISI*) were
296 assessed in comparison with their estimation for the basic *NS* model in the first row of Table
297 1. Therefore, it may be concluded that the simulation design achieved the general goal for
298 inducing stronger synchronization between MU firings. More details on the observed MU
299 synchronizations related to the computation of *corMU* and *CISI* are presented below.

- 300 • *corMU*: Different effects of the synchronization induced by Methods 1 through 4 could
301 be tracked well on the *corMU* color map (Figs. 5B–5E), seen as clusters with strong
302 correlations (*corMU* is from 30% to 100%). These clusters have different two-
303 dimensional space distributions of the entries with maximal correlation,
304 corresponding to the different concepts for synchronization of MU pairs in Methods
305 1 through 4, as follows:
- 306 ○ *Method 1*: The synchronization between neighboring MUs is seen in Fig. 5B as
307 maximal correlations around the main diagonal (identical MUs and their closer
308 neighbors) and a trend of gradually decreasing correlations moving away from
309 that diagonal (MU pairs with far neighborhood). Three clusters with *corMU*
310 gradient can be identified in Fig. 5B as a result of synchronization within MUs
311 of the same physiological type (S–S, FR–FR, FF–FF). Within these clusters, the
312 maximal correlation (mean value \pm standard deviation) is observed for FR MUs
313 (38.4% \pm 21.1%), S MUs (37.2% \pm 19.5%), and minimally for FF MUs (22.3%
314 \pm 22.4%), considering the setting with a maximal synchronization interval $\Delta t = \pm$
315 6 ms (Table 1). This means up to 30% increase in the correlation coefficients
316 within MU groups, as compared with in the basic *NS* model.
- 317 ○ *Method 2*: The synchronization was applied to not ordered MU pairs within the
318 same physiological type; therefore, the *corMU* color map in Fig. 5C appears with
319 a non ordered colorful distribution with strong correlations between various MU
320 pairs, forming three clusters within MUs from the same physiological type (S–S,
321 FR–FR, FF–FF). Within these clusters, maximal correlation (mean value \pm
322 standard deviation) was observed for FR MUs (39.7% \pm 21.5%), S MUs (38.1%
323 \pm 19.7%), and minimally for FF MUs (20.2% \pm 21.9%), considering the setting

324 with a maximal synchronization interval $\Delta t = \pm 6$ ms (Table 1). We note that the
325 reported average *corMU* values in Method 2 are very similar to those in Method
326 1. Considering that both methods had a common concept for MU
327 synchronization in pairs, we could deduce that the synchronization concept and
328 not the order of MU recruitment can help in increasing the synchronization index
329 by up to 30%, although the effect on the output force is expected to be different.

- 330 ○ *Method 3*: The synchronization between unique groups of four neighboring MUs
331 is seen in Fig. 5D as maximal correlations in clusters with (4×4) entries,
332 distributed around the main diagonal (including the identical MU pair and its
333 three closest neighbors). There are two exceptions with smaller clusters,
334 including 3×3 entries (MU numbers 29, 30, 31) and 2×2 entries (MU numbers
335 56, 57), which exactly correspond to the methodological constraints. Considering
336 all MUs within the same physiological type, the maximal correlation (mean
337 value \pm standard deviation) is estimated for S MUs ($15.7\% \pm 14.8\%$), FR MUs
338 ($13.5\% \pm 16.2\%$), and minimally for FF MUs ($9.9\% \pm 13.9\%$) in the setting with
339 a maximal synchronization interval $\Delta t = \pm 6$ ms (Table 1). This result yields an
340 increment of 6% to 18% of *corMU* after Method 3 synchronization relative to
341 with the basic *NS* model. In general, Method 3 induces a smaller level of
342 synchronization than Methods 1 and 2, which can be deduced from the larger
343 size of the dark blue color area with uncorrelated MU pairs found in Fig. 5D as
344 compared with in Figs. 5B and 5C.
- 345 ○ *Method 4*: The concept for synchronization of all MUs within the same
346 physiological type to only one reference MU resulted in MU clusters with very
347 high pairwise correlations, enclosing all MUs in the respective physiological

348 type (S–S, FR–FR, FF–FF). Within these clusters, the maximal correlation
349 (mean value \pm standard deviation) was observed for FR MUs (74.6% \pm 6.9%),
350 FF MUs (62.8% \pm 13.1%), and minimally for S MUs (42.6% \pm 10.9%) in the
351 setting with a maximal synchronization interval $\Delta t = \pm 6$ ms (Table 1). This
352 result yields an increment from 37% to 67% of the correlations within MU
353 groups relative to with the basic *NS* model and can be denoted as the maximal
354 synchronization level simulated in this study.

355 • *CISI*: The effect of synchronization induced by Methods 1 through 4 could be
356 identified in the cross-interval histograms (Figs. 6B–6E) by the prominent peak in the
357 central bin (± 0.5 ms). The larger is amplitude deviation from the uniform distribution
358 in other bins, the higher the probability for synchronization of the respective MU to
359 the firing pulses of other MUs. Different synchronization methods produce different
360 amplitudes in the central bin, estimated by *CISI* in Table 1. Comparing the *CISI*
361 values of all methods estimated with maximal synchronization interval $\Delta t = \pm 6$ ms,
362 we could deduce the following:

- 363 ○ The lowest *CISI* mean value was found for S MUs (from 8.2% in Method 3 to
364 10.3% in Method 2, with the latter being up to 4.5% above the basic *NS* model).
- 365 ○ The largest *CISI* mean value was found for both FF MUs (from 9% in Method 3
366 to 31.6% in Method 4) and FR MUs (from 9.7% in Method 3 to 32.1% in
367 Method 4). Thus, the best synchronization of Method 4 achieved up to a 25.9%
368 greater *CISI* value as compared with the basic *NS* model.

369 Additionally, Fig. 8A was designed to show the effect of widening the time window for
370 synchronization ($\Delta t = \pm 2, \pm 4,$ and ± 6 ms) on the relative *CISI* change (ratio of synchronized

371 vs. *NS* value). It shows that, generally, $\Delta t = \pm 2$ ms leads to weak synchronization and slight
372 increases in *CISI* by about 1.1 times (Methods 1–3) and 1.8 times (Method 4); $\Delta t = \pm 4$ ms
373 lead to maximal synchronization that is still less than two times (Methods 1–3) but about
374 three times (Method 4); and $\Delta t = \pm 6$ ms produced the maximal synchronization with notable
375 *CISI* increment increases by up to three times (Methods 1 and 2) and up to five times
376 (Method 4).

377 ***Maximal effect of MU synchronization on the force parameters***

378 The forces produced by the muscle and different MU types before and after the application of
379 different synchronization scenarios were estimated for a two -second period during the
380 muscle steady state and the defined five basic force parameters (*meanF*, *rmsF*, *rangeF*,
381 *maxF*, and *meanfreq*) are presented in Table 2. For comprehension purposes, the
382 representation of those parameters on the force signals and their PSD is additionally
383 illustrated in Fig. 7. The comparison of the *NS* excitation to those achieved with different
384 synchronization methods (Methods 1–4) is presented below.

- 385 • *Force mean value*: The synchronization had no effect on *meanF* value, showing a
386 negligible change (≤ 12 mN) before and, after the synchronization was applied, i.e.,
387 for the muscle force, *meanF* was varying from 4052 mN (*NS*) to a maximum of 4064
388 mN (Method 4, $\Delta t = \pm 6$ ms) (Table 2). This can be also tracked in Fig. 7A, which
389 presents no visible difference in the baseline value (red solid horizontal line) when
390 comparing all forces placed in a row.
- 391 • *Force RMS value*: The synchronization had an important effect on increasing the
392 *rmsF* value by more than 50 mN, which could become as high as 129 mN for the
393 muscle force (Method 4, $\Delta t = \pm 6$ ms), considering its baseline *NS* value of 73.5 mN

394 (Table 2). Additionally, Fig. 8B is provided to show the relative *rmsF* change as a
395 ratio of synchronized vs. *NS* value. Specifically, it shows that the maximal *rmsF*
396 increment (about two times) could be achieved for the forces of two types of MUs (S,
397 FR) following synchronization with Methods 1, 2, and 4, $\Delta t = \pm 6$ ms. Considering the
398 whole muscle, the observed maximal increment of *rmsF* was about 1.8 times,
399 achieved using Method 4, $\Delta t = \pm 6$ ms.

400 • *Force min–max range*: The synchronization had an important effect on increasing the
401 *rangeF* value by about 450 mN, which increased from 405 mN (*NS*) up to 850 mN
402 for the muscle force after synchronization with Method 4, $\Delta t = \pm 6$ ms (Table 2). The
403 *rangeF* ratio (synchronized vs. *NS* value) in Fig. 8C shows that the largest *rangeF*
404 increment (two to 2.6 times) was achieved for the forces of two types of MUs (S, FR)
405 after synchronization with Methods 1, 2 and 4, $\Delta t = \pm 6$ ms. Considering the whole
406 muscle, the observed maximal increment of *rangeF* (about 2.1 times) was with
407 Method 4, $\Delta t = \pm 6$ ms. Although the observations concerning *rangeF* are similar to
408 those of *rmsF* as was noted above, the relative and absolute changes in *rangeF* values
409 as an effect of synchronization were larger. This could also be visually confirmed by
410 the force signals in Fig. 7A (blue dotted lines show larger span than red dotted lines
411 after synchronization, comparing all forces placed in a row).

412 • *Maximal force*: The synchronization had an important effect on increasing the *maxF*
413 value by more than 205 mN, which could raise it from 4234 mN (*NS*) up to 4440 mN
414 for the muscle force after synchronization with Method 4, $\Delta t = \pm 6$ ms (Table 2). The
415 *maxF* ratio (synchronized vs. *NS* value) in Fig. 8D shows that the largest *maxF*
416 increment (up to 1.7 times) is achieved for the forces of two types of MUs (FR, FF)
417 after synchronization with Method 4 or Method 1, $\Delta t = \pm 6$ ms. Considering the whole

418 muscle, the observed maximal increment of $maxF$ was about 1.5 times using Method
419 4, $\Delta t = \pm 6$ ms. This relative change of $maxF$ was found to be smaller than the force
420 amplitude variations estimated above by the other two force parameters ($rangeF$ and
421 $rmsF$).

422 • *Force mean spectral frequency:* In this context, the synchronization had an important
423 effect—decreasing the $meanfreq$ value by more than 10 Hz, which drops it from 35.6
424 Hz (*NS*) down to 24.4 Hz for the muscle force after synchronization with Method 4,
425 $\Delta t = \pm 6$ ms (Table 2). The $meanfreq$ ratio (synchronized vs. *NS* value) in Fig. 8E
426 shows that the largest $meanfreq$ drop (i.e., < 0.75 or $> 25\%$ vs. *NS*) could be achieved
427 for the forces of two types of MUs (S, FF) after synchronization with Methods 1, 2
428 and 4, $\Delta t = \pm 6$ ms. Considering the whole muscle, the observed maximum drop of
429 $meanfreq$ was about 30% (< 0.7 Hz) with Method 4, $\Delta t = \pm 6$ ms. This can be
430 observed in the *PSD* of Fig. 7B (first row for the muscle force and second row for FF
431 MU force) as a shift of the high-frequency components (predominantly around 40 Hz)
432 in the *NS* spectrum to low-frequency components (10–25 Hz) in the spectrum for
433 synchronization with Method 4, $\Delta t = \pm 6$ ms.

434 ***Correlation of the force variance and MU synchronization***

435 The results presented in this section aim to answer the general question of whether the
436 provided synchronization methods regularized by widening the time window for
437 synchronization ($\Delta t = \pm 2, \pm 4, \text{ and } \pm 6$ ms) led to consistent increases in both the level of MU
438 synchronization (*CISI*) and the induced changes in the force output. Thus, the force
439 parameters, which were most closely correlated to the synchronization design in Methods 1
440 through 4, could be deduced. The results in Table 3 establish the correlations between the

441 curves in Fig. 8A for the level of MU synchronization in the function of Δt ($CISI = f(\Delta t)$) and
442 each of the curves in Figs. 8B through 8E for the variance of the five force parameters as a
443 function of Δt ($meanF$, $rmsF$, $rangeF$, $maxF$, $meanfreq$). The correlations were estimated in
444 the range $[-1;+1]$, where +1 and -1 stand for strongly correlated curves that were directly or
445 inversely proportional, respectively. The results show that $rmsF$, $rangeF$ and $maxF$ were the
446 most robust force parameters, which were consistently increased by the synchronization level
447 with an average correlation coefficient of 0.97; the force mean spectral frequency was indeed
448 inversely proportional to the synchronization level, with an average correlation coefficient of
449 -0.89; and $meanF$ was the parameter least dependent on the synchronization, with an average
450 correlation coefficient of 0.53.

451

452 **Discussion**

453 There are two different approaches one could use to investigate the synchrony between
454 different MUs and its influence on the developed muscle force. The first one involves
455 assessing experimental recordings of electromyographic signals using needle or surface
456 electrodes and decomposing these signals into individual action potentials [4, 37-40].
457 However, the disadvantages of this approach include that only a portion of the active MUs is
458 recorded, it is not possible to distinguish fast from slow MUs and the measured muscle force
459 reflects the force of all active MUs, and even MUs of other muscles. The second method is
460 based on pure modeling, wherein models of the muscle are composed using different MUs
461 [21, 31]. These models are based on the Fuglevand et al. approach [30] and contain 120 MUs.
462 However, these authors did not divide MUs into different types (S, FR, and FF). Moreover,
463 the function used for describing the twitch was based only on two parameters: force
464 amplitude and contraction time. The model used in the current paper, constructed based on

465 experimental data concerning MU twitch and tetanus properties as well as motoneuronal
466 excitability, has been fully described previously [33]. Here, the experimentally measured
467 twitches are modeled by a six-parameter function and the summation of the twitches into
468 tetanus is established by an experimentally verified mathematical algorithm. In the adopted
469 basic model, it was proven that the firing of all MUs is asynchronous. Then, synchronization
470 was imposed in this basic MU firing arrangement, changing the pattern of impulses of MUs
471 during the steady state of the muscle force using several simulated situations (i.e., four modes
472 of synchronization with the three time windows ± 2 , ± 4 , and ± 6 ms). In this way, broad
473 investigation of the influence of the synchrony of the three types of the MUs on the
474 developed muscle force and cumulative forces of MUs from the three groups could be
475 performed. The results based on the two used coefficients *corMU* and *CISI* showed that the
476 range, the maximum, and the root-mean-square of the forces rose with increased
477 synchronization, while the mean forces remained nearly unchanged. This increase was
478 stronger for fast MUs; notably, these units are mostly responsible for the force instability
479 (muscle tremor) in the context of moderate or strong muscle contractions, wherein fast MUs
480 are recruited into activity.

481 ***Models of MU synchronization***

482 To increase the degree of synchronization and to analyze its effects on the muscle and MU
483 forces, we considered the synchronization of pulses of pairs of MUs in the time windows ± 2 ,
484 ± 4 , and ± 6 ms. It is known that synchronization is an effect of a common excitatory input to
485 several motoneurons and that synchronic excitatory postsynaptic potentials (EPSPs) evoked
486 in several motoneurons increase the probability of the simultaneous occurrence of their action
487 potentials [41]. The size of the time windows is related to the duration of EPSPs in rat
488 motoneurons, lasting several milliseconds, with an increasing phase often remaining below 2

489 ms (for example, for Ia monosynaptic EPSPs, see Fig. 1 in Seburn and Cope [42].
490 Additionally, the applied method resulted in a narrow peak in the cross-interval histogram
491 (Fig. 6), similar to that reported for human muscles by De Luca et al. [4], as is typical for
492 short-term synchronization (i.e., the peak centered about zero-time delay 0.5 ± 2.9 ms) and
493 with an average width of 4.5 ± 2.5 ms. For all four proposed modes of synchronization used
494 in the present study, the same range of time windows was applied. The largest (± 6 ms) time
495 window increased the *CISI* by about 1.5 times for Method 1, about 2.5 times for Methods 2
496 and 3, and more than three times for Method 4 (see Table 1). The range of differences in the
497 obtained synchronization is similar to that of differences in the *CISI* reported for trained and
498 nontrained subjects (more than two times higher in weightlifters), changes resulting from
499 conditioning exercise (about 2.5 times higher after the exercise), and those between dominant
500 and nondominant hands (1.6 times higher in the nondominant hand) [39].

501 The proposed method of inducing synchronization within time windows Δt of variable
502 duration appeared to be an efficient tool in the four tested simulations. For all four methods
503 of synchronization, values of the investigated parameters *musF*, *rangeF*, and *maxF*, which
504 characterized the force oscillations, rose along with increases in the time window Δt , i.e.,
505 when the synchronization degree was augmented (Fig. 8). Notably, this increase appeared
506 strongest with Method 4 and weakest with Method 3. Meanwhile, the highest value of *corMU*
507 (74.6) was achieved for $\Delta t = \pm 6$ ms for FR MUs (Table 1). Moreover, except for in Method
508 3, the highest values of *corMU* were observed for FR MUs (Table 1). This observation is
509 surprising in light of previous physiological experiments concerning force
510 decreases/increases resulting from the prolongation/shortening of one IPI during the unfused
511 tetanic contraction ascertained using MUs of the rat medial gastrocnemius [28]. Namely,
512 relative force fluctuations noted for FF and FR MUs were similar and one could expect no

513 differences to exist between these two types of fast MUs in the present simulation study. This
514 methodological approach resulted in the highest synchronization for Method 4 and is
515 reflected by the parameters *corMU* and *CISI* in Table 1. It should be stressed that the four
516 methods led to similar effects on muscle force—that is, greater maximal force and higher
517 fluctuations around a mean force—and these increases concerned all three types of MUs,
518 although it should be stressed that this result was obtained for the maximum excitation signal,
519 i.e., a simulation of a very strong contraction, when all MUs were active.

520 *Effects of synchronization on MU and muscle forces*

521 The influence of the increasing synchronization level on the mean as well as on the
522 maximum force of particular MU types and of the whole muscle was, in general, very weak
523 (i.e., the maximum force increased by up to 5% for the whole muscle and up to 7% for FF
524 MUs), regardless of the synchronization method applied in the model. This confirms the
525 results of previous studies, which also demonstrated that the magnitude of force output and
526 the average force of the muscle were not altered considerably due to synchronization [21, 39].
527 However, an increase in the synchronization time window from ± 2 to ± 6 ms in all cases
528 correlated with a rise in the force of each MU type, with the change being the greatest for
529 synchronization Methods 1 and 4. Moreover, the present study has revealed certain
530 differences between MU types. Not only did the absolute force increase but also the relative
531 force increased after synchronization; further, they were always the highest for fast MUs (FF
532 and FR) and the lowest for slow MUs. This also confirms previous observations that
533 synchronization may be beneficial during the performance of contractions where rapid force
534 development is required, for which fast MUs should be recruited [17].

535 On the other hand, it was already mentioned that a muscle can produce smooth
536 contractions due to asynchronous discharges of motor neurons [17, 23] and that

537 synchronization increases the variability in the muscle force [21]. Indeed, simulated
538 contractions in our model have confirmed that synchronization substantially influences the
539 range of force oscillations during the steady state of the muscle contraction and the min–max
540 range of modeled forces gradually rose with the increase in the time window for
541 synchronization in each method. This can be partly explained by previous computer
542 simulations indicating that synchronization leads to an increase in the estimated twitch force
543 and to a decrease in the estimated contraction time of an MU [26]. Obviously, absolute values
544 of the min–max range of the force were the lowest for the weakest S MUs, but the ratio of the
545 $rangeF$ parameters (as well as the ratio of the $rmsF$ parameters) between synchronized and
546 NS models was the highest for S MUs for all methods—except Method 4, in which MUs of
547 the same type were synchronized according to the first MU in the group (see Figs. 8B and
548 8C).

549 A 100% excitation signal (corresponding to a very strong muscle contraction) used in
550 this model was applied to ensure activation of all MU types, which helped us to elucidate the
551 contributions of the three types of MUs to muscle tremor, which are dependent on the force
552 level [43]. According to the size principle, at a lower excitation signal, a contribution of high-
553 threshold fast MUs (especially those of the FF type) to the force development would be
554 smaller or recruitment would be restricted to low-threshold (S or S and FR) MUs. The lowest
555 relative force oscillations were noted in FF MUs for all methods of synchronization (Fig. 8B).
556 This observation indicates that slow MUs have the strongest and FF MUs have the weakest
557 relative influence, respectively, on force fluctuations described as muscle tremor and thus
558 partly explains why tremor is best visible during weak contractions, when predominantly
559 slow MUs are recruited.

560

561 ***The influence of synchronization on the spectral frequency of the muscle force***

562 To our knowledge, the parameter *meanfreq* of the force has not been analyzed in
563 muscle modeling in connection with the synchronization of MU firing to date. It should be
564 noted, however, that the power spectral analysis of tremor in the first dorsal interosseous
565 muscle revealed three frequency peaks occurring at around 10 Hz, 20 Hz, and 40 Hz [24],
566 which correspond to our findings concerning the mean spectral frequencies of S, FR, and FF
567 MUs, respectively (Table 2). McAuley et al. [24] concluded that their results reflected the
568 synchronization of MUs at frequencies determined by oscillations within the central nervous
569 system; however, our findings suggest that the force oscillations related to three types of
570 MUs likely contribute to those frequency peaks.

571 A decrease in the *meanfreq* was observed in parallel with an increase in the degree of
572 synchronization in all four applied methods. It should be stressed that the mean firing
573 frequencies of all MUs remained unchanged during simulations, due to a constant number of
574 pulses in the analyzed time window (2000 ms). A decrease in force spectral frequencies
575 paired with the occurrence of slower force oscillations. This observation at increased
576 synchronization levels indicates that the force-frequency spectrum depends upon the temporal
577 distribution rather than on the mean firing frequencies of MUs and this conclusion concerns
578 all three types of MUs, despite considerable differences in the *meanfreq* between S, FR, and
579 FF MUs. The decrease in the *meanfreq* could not be linked to muscle fatigue, which was not
580 modeled, and should instead be connected with processes of summation of twitches into
581 tetanic contractions.

582 McAuley and Marsden [44] in their review argued that the physiological tremor in
583 humans is likely of multifactorial origin, with contributions from the 10-Hz range of
584 oscillatory activity of the central nervous system, MU discharge frequencies, reflex loop

585 resonances, and mechanical resonances. However, it must be emphasized that the present
586 results were obtained using the model of a rat muscle, so it is risky to directly compare the
587 frequencies related to different types of MUs collected herein to human data, most of all
588 because rat MUs demonstrate considerably faster contractions and have higher discharge
589 frequencies.

590 ***Conclusion***

591 The present study revealed that, regardless of the method used for the synchronization of MU
592 firings, the increase in the synchronization index had a negligible effect on the mean force of
593 the developed contractions yet influenced muscle tremor by increasing force oscillations and
594 further highlighted that these results were observed for all three types of MUs. A parallel
595 decrease in the mean spectral frequency of the force indicated that, in the synchronized
596 models, the force oscillations were slower despite higher magnitudes. The synchronization of
597 fast MUs led to higher increases in the range of the force variability and the force root-mean-
598 square in comparison with that of slow MUs. On the other hand, relative changes in the latter
599 parameters in the synchronized simulations were the highest for slow MUs, indicating their
600 significant contribution to muscle tremor, especially during weak contractions.

602 **Acknowledgments**

603 The study was supported by a bilateral agreement between the Bulgarian Academy of
604 Sciences and the Polish Academy of Sciences.

605

606 **Author contributions**

607 Conceptualization: RR, JC, PK

608 Data curation: RR, VK

609 Formal analysis: RR, VK, PK, JC

610 Funding acquisition: RR, JC

611 Investigation: RR, VK, PK, HDC, KK, JC

612 Project administration: RR, JC

613 Software: RR, VK

614 Validation: RR, VK, PK

615 Writing—original draft: RR, VK, PK, JC, KK

616 Writing—review and editing: RR, VK, PK, HDC, KK, JC

617

619 **References**

- 620 1. Datta AK, Stephens JA. Synchronization of motor unit activity during voluntary
621 contraction in man. *J Physiol.* 1990;422:397-419.
- 622 2. Kutch JJ, Suresh NL, Bloch AM, Rymer WZ. Analysis of the effects of firing rate and
623 synchronization on spike-triggered averaging of multidirectional motor unit torque. *J Comput*
624 *Neurosci.* 2007;22(3):347-361.
- 625 3. Keen DA, Chou LW, Nordstrom MA, Fuglevand AJ. Short-term synchrony in diverse
626 motor nuclei presumed to receive different extents of direct cortical input. *J Neurophysiol.*
627 2012;108(12):3264-3275.
- 628 4. De Luca CJ, Roy AM, Erim Z. Synchronization of motor-unit firings in several human
629 muscles. *J Neurophysiol.* 1993;70(5):2010-2023.
- 630 5. Kirkwood PA, Sears TA, Stagg D, Westgaard RH. The spatial distribution of
631 synchronization of intercostal motoneurons in the cat. *J Physiol.* 1982;327:137-155.
- 632 6. Schmied A, Ivarsson C, Fetz EE. Short-term synchronization of motor units in human
633 extensor digitorum communis muscle: relation to contractile properties and voluntary control.
634 *Exp Brain Res.* 1993;97(1):159-172.
- 635 7. Semmler JG, Nordstrom MA. Influence of handedness on motor unit discharge properties
636 and force tremor. *Exp Brain Res.* 1995;104(1):115-125.
- 637 8. Sears TA, Stagg D. Short-term synchronization of intercostal motoneurone activity. *J*
638 *Physiol.* 1976;263(3):357-381.
- 639 9. Farina D, Negro F. Common synaptic input to motor neurons, motor unit synchronization,
640 and force control. *Exerc Sport Sci Rev.* 2015;43(1):23-33.

- 641 10. Kirkwood PA. On the use and interpretation of cross-correlations measurements in the
642 mammalian central nervous system. *J Neurosci Methods*. 1979;1(2):107-132.
- 643 11. Nordstrom MA, Fuglevand AJ, Enoka RM. Estimating the strength of common input to
644 human motoneurons from the cross-correlogram. *J Physiol*. 1992;453:547-574.
- 645 12. Datta AK, Farmer SF, Stephens JA. Central nervous pathways underlying
646 synchronization of human motor unit firing studied during voluntary contractions. *J Physiol*.
647 1991;432:401-425.
- 648 13. Adams L, Datta AK, Guz A. Synchronization of motor unit firing during different
649 respiratory and postural tasks in human sternocleidomastoid muscle. *J Physiol*. 1989;
650 413:213-231.
- 651 14. Kim MS, Masakado Y, Tomita Y, Chino N, Pae YS, Lee KE. Synchronization of single
652 motor units during voluntary contractions in the upper and lower extremities. *Clin*
653 *Neurophysiol*. 2001;112(7):1243-1249.
- 654 15. Bremner FD, Baker JR, Stephens JA. Effect of task on the degree of synchronization of
655 intrinsic hand muscle motor units in man. *J Neurophysiol*. 1991;66(6):2072-2083.
- 656 16. Huesler EJ, Hepp-Reymond MC, Dietz V. Task dependence of muscle synchronization in
657 human hand muscles. *Neuroreport*. 1998;9(10):2167-2170.
- 658 17. Semmler JG, Nordstrom MA. Motor unit discharge and force tremor in skill- and
659 strength-trained individuals. *Exp Brain Res*. 1998;119(1):27-38.
- 660 18. Sturm H, Schmied A, Vedel JP, Pagni S. Firing pattern of type-identified wrist extensor
661 motor units during wrist extension and hand clenching in humans. *J Physiol*. 1997;504 (Pt
662 3):735-745.

- 663 19. Milner-Brown HS, Stein RB, Lee RG. Synchronization of human motor units: possible
664 roles of exercise and supraspinal reflexes. *Electroencephalogr Clin Neurophysiol.*
665 1975;38(3):245-254.
- 666 20. Schmied A, Pagni S, Sturm H, Vedel JP. Selective enhancement of motoneurone short-
667 term synchrony during an attention-demanding task. *Exp Brain Res.* 2000;133(3):377-390.
- 668 21. Yao W, Fuglevand RJ, Enoka RM. Motor-unit synchronization increases EMG amplitude
669 and decreases force steadiness of simulated contractions. *J Neurophysiol.* 2000;83(1):441-
670 452.
- 671 22. Lippold OC, Redfearn JW, Vuco J. The rhythmical activity of groups of motor units in
672 the voluntary contraction of muscle. *J Physiol.* 1957;137(3):473-487.
- 673 23. Dietz V, Bischofberger E, Wita C, Freund HJ. Correlation between the discharges of two
674 simultaneously recorded motor units and physiological tremor. *Electroencephalogr Clin*
675 *Neurophysiol.* 1976;40(1):97-105.
- 676 24. McAuley JH, Rothwell JC, Marsden CD. Frequency peaks of tremor, muscle vibration
677 and electromyographic activity at 10 Hz, 20 Hz and 40 Hz during human finger muscle
678 contraction may reflect rhythmicities of central neural firing. *Exp Brain Res.*
679 1997;114(3):525-541.
- 680 25. Halliday DM, Conway BA, Farmer SF, Rosenberg JR. Load-independent contributions
681 from motor-unit synchronization to human physiological tremor. *J Neurophysiol.*
682 1999;82(2):664-675.
- 683 26. Taylor AM, Steege JW, Enoka RM. Motor-unit synchronization alters spike-triggered
684 average force in simulated contractions. *J Neurophysiol.* 2002;88(1):265-276.

- 685 27. Kernell D, Eerbeek O, Verhey BA. Relation between isometric force and stimulus rate in
686 cat's hindlimb motor units of different twitch contraction time. *Exp Brain Res.* 1983; 50(2-
687 3):220-227.
- 688 28. Celichowski J, Grottel K. Sensitivity of the motor unit unfused tetanus to changes in the
689 pattern of motoneuronal firing. *Arch Ital Biol.* 2001;139(4), 329-336.
- 690 29. Grottel K, Celichowski J. The influence of changes in the stimulation pattern on force and
691 fusion in motor units of the rat medial gastrocnemius muscle. *Exp Brain Res.*
692 1999;127(3):298-306.
- 693 30. Fuglevand AJ, Winter DA, Patla AE. Models of recruitment and rate coding organization
694 in motor-unit pools. *J Neurophysiol.* 1993;70(6):2470-2488.
- 695 31. Santello M, Fuglevand AJ. Role of across-muscle motor unit synchrony for the
696 coordination of forces. *Exp Brain Res.* 2004;159(4):501-508.
- 697 32. Raikova R, Aladjov H, Celichowski J, Krutki P. An approach for simulation of the
698 muscle force modeling it by summation of motor unit contraction forces. *Computational and*
699 *Mathematical Methods in Medicine*, 2013 Vol. 2013, Article ID 625427.
- 700 33. Raikova R, Celichowski J, Angelova S, Krutki P. A model of the rat medial
701 gastrocnemius muscle based on inputs to motoneurons and on an algorithm for prediction of
702 the motor unit force. *J Neurophysiol.* 2018;120(4):1973-1987.
- 703 34. Raikova R, Pogrzebna M, Drzymala H, Celichowski J, Aladjov H. Variability of
704 successive contractions subtracted from unfused tetanus of fast and slow motor units. *J*
705 *Electromyogr Kinesiol.*, 2008;18(5):741-751.

- 706 35. De Luca CJ, Erim Z. Common drive of motor units in regulation of muscle force. Trends
707 Neurosci. 1994;17(7):299-305.
- 708 36. Raikova R., Celichowski J, Krutki P. A general mathematical algorithm for predicting the
709 course of unfused tetanic contractions of motor units in rat muscle. Plos One. 2016
710 11(9):e0162385.
- 711 37. Loeb GE, Yee WJ, Pratt CA, Chanaud CM. Cross-correlation of EMG reveals widespread
712 synchronization of motor units during some slow movements in intact cats. J Neurosci
713 Method. 1987: 239-249.
- 714 38. Kline JC, De Luca CJ. Synchronization of motor unit firings: an epiphenomenon of firing
715 rate characteristics not common inputs. J Neurophysiol. 2016;115(1):178-192.
- 716 39. Semmler JG. Motor unit synchronization and neuromuscular performance. Exerc. Sport
717 Sci. Rev. 2002;30(1):8-14.
- 718 40. Logigian EL, Wierzbicka MM, Bruyninckx F, Wiegner AW, Shahahi BT, Young RR.
719 Motor unit synchronization in physiologic, enhanced physiologic and voluntary tremor in
720 man. Ann Neurol 1988 Mar;23(3):242-250.
- 721 41. Gallego JA, Dideriksen JL, Holobar A, Ibáñez J, Pons JL, Louis ED, Rocon E, Farina D.
722 Influence of Common Synaptic Input to Motor Neurons on the Neural Drive to Muscle in
723 Essential Tremor. J Neurophysiol. 2015;113(1):182-191.
- 724 42. Seburn KL, Cope TC. Short-term afferent axotomy increases both strength and
725 depression at Ia–motoneuron synapses in rat. J Neurosci. 1998;18(3):1142-1147.
- 726 43. Novak T, Newell KM. Physiological Tremor (8-12 Hz Component) in Isometric Force
727 Control. Neurosci Lett. 2017;641:87-93.

- 728 44. McAuley J H, Marsden CD. Physiological and pathological tremors and rhythmic central
729 motor control. *Brain*, 2000, 123 (8): 1545–1567.

731

		corMU [%]				CISI [%]			
		S MUs	FR MUs	FF MUs	all MUs	S MUs	FR MUs	FF MUs	all MUs
	NS	4.5±2.0	7.4±2.9	5.7±2.8	6.1±2.8	5.8±0.5	6.2±0.4	6.2±0.3	6.2±0.4
Method 1	±2ms	10.4±7.8	11.5±8.6	8.2±7.6	7.3±5.8	6.4±0.8	7.8±0.6	7.3±0.7	7.4±0.8
	±4ms	21.9±15.2	21.3±16.5	13.4±14.7	10.2±11.4	8.1±0.9	11.7±0.9	9.6±1.6	10.3±1.8
	±6ms	37.2±19.5	38.4±21.1	22.3±22.4	15.0±18.4	8.8±1.0	18.7±1.8	13.9±3.4	15.1±4.3
Method 2	±2ms	10.4±9.7	11.4±10.6	8.4±9.0	7.6±6.6	6.7±0.5	8.0±1.0	7.6±0.8	7.6±0.9
	±4ms	20.6±15.7	22.5±19.0	13.9±15.9	10.5±12.5	7.6±0.5	12.3±1.8	10.0±1.8	10.6±2.3
	±6ms	38.1±19.7	39.7±21.5	20.2±21.9	15.2±18.4	10.3±0.8	19.4±3.1	13.3±2.9	15.4±4.5
Method 3	±2ms	9.5±7.7	10.0±7.9	7.5±7.5	6.9±5.4	6.4±0.6	7.2±0.4	6.9±0.7	6.9±0.6
	±4ms	15.7±14.8	13.5±16.2	9.9±13.9	7.9±9.9	7.2±0.8	8.4±0.5	7.9±1.2	8.0±1.0
	±6ms	23.8±23.5	16.8±24.3	12.2±20.0	9.1±14.5	8.2±1.0	9.7±0.7	9.0±1.4	9.2±1.2
Method 4	±2ms	11.5±6.9	19.5±7.6	16.6±9.3	10.1±8.2	6.3±0.7	10.8±1.6	10.9±1.9	10.2±2.3
	±4ms	24.9±10.6	46.6±9.6	39.3±13.5	19.1±19.5	7.8±1.1	21.4±2.1	21.0±2.4	19.3±5.2
	±6ms	42.6±10.9	74.6±6.9	62.8±13.1	28.3±31.2	9.0±1.4	32.1±1.5	31.6±1.4	28.6±8.1

732

733

734 **Table 1.** Two indices of synchronization (*corMU* and *CISI*), measured for the *NS* model and four
735 methods of synchronization (Methods 1–4) within three time windows (± 2 , ± 4 , and ± 6 ms). All
736 values are reported as the mean value \pm standard deviation for different physiological types of MUs
737 (S, FR, and FF) and for all MUs within the muscle.

739

	S	FR	FF	muscle	S	FR	FF	muscle	S	FR	FF	muscle	
	meanF [mN]				rmsF [mN]				rangeF [mN]				
	NS	385	1449	2219	4052	3.2	27.2	71.2	73.4	16.8	146	395	405
Method 1	±2ms	385	1449	2217	4051	3.7	28.9	71.8	75.4	17.8	147	434	415
	±4ms	385	1449	2218	4052	5.0	38.9	81.4	87.2	26.0	222	511	606
	±6ms	385	1453	2228	4066	6.9	54.5	103	116	37.7	314	564	620
Method 2	±2ms	385	1449	2218	4052	3.6	28.7	73.6	77.4	19.8	147	427	465
	±4ms	385	1449	2226	4059	5.0	39.4	81.9	89.9	24.5	250	518	533
	±6ms	385	1450	2226	4061	6.5	44.9	93.8	101	38.8	287	560	624
Method 3	±2ms	385	1448	2218	4051	3.5	28.9	72.0	75.8	21.1	165	434	462
	±4ms	385	1448	2216	4049	4.4	35.2	79.2	79.7	25.3	195	568	472
	±6ms	385	1447	2223	4057	5.5	44.0	98.1	103	34.4	274	603	687
Method 4	±2ms	385	1449	2218	4052	3.3	28.8	70.1	73.1	19.7	160	431	487
	±4ms	385	1451	2217	4051	4.5	40.1	79.1	88.9	25.7	257	508	599
	±6ms	385	1458	2224	4064	6.1	56.0	110	129	31.6	397	714	850
	maxF [mN]				mean freq [Hz]								
	NS	393	1519	2398	4234	13.6	24.0	36.1	35.6				
Method 1	±2ms	395	1523	2406	4239	12.6	23.8	35.7	34.1				
	±4ms	399	1557	2457	4357	11.3	22.6	33.1	31.5				
	±6ms	402	1627	2460	4370	10.2	22.7	32.2	31.5				
Method 2	±2ms	394	1517	2407	4258	12.9	24.0	35.7	34.2				
	±4ms	397	1586	2456	4316	10.9	20.7	33.1	30.9				
	±6ms	402	1588	2482	4367	10.4	23.6	29.8	30.0				
Method 3	±2ms	395	1531	2407	4259	13.3	24.1	35.7	34.4				
	±4ms	399	1544	2462	4256	12.1	22.4	33.2	33.9				
	±6ms	404	1574	2517	4330	11.5	21.6	30.8	31.2				

Method 4	±2ms	394	1523	2399	4250	13.4	23.8	35.5	34.6
	±4ms	398	1587	2472	4331	10.8	21.2	32.3	29.5
	±6ms	399	1626	2565	4440	10.8	21.6	25.9	24.4

740

741 **Table 2.** Estimation of the five force parameters $meanF$, $rmsF$, $rangeF$, $maxF$, and $meanfreq$ of
742 different physiological types of MUs (S, FR, and FF) and the whole muscle, produced by the *NS* model
743 and four methods for synchronization (Methods 1–4), within three time windows (± 2 , ± 4 , and ± 6
744 ms).

746

747

Force parameters	Method 1				Method 2				Method 3				Method 4			
	S	FR	FF	all	S	FR	FF	all	S	FR	FF	all	S	FR	FF	all
meanF	-0.30	0.93	0.89	0.90	-0.36	0.88	0.88	0.90	0.13	0.70	0.57	0.57	-0.51	0.84	0.73	0.78
rmsF	0.96	1.00	0.99	0.99	0.98	0.96	1.00	0.99	0.99	0.98	0.94	0.91	0.98	0.99	0.92	0.95
rangeF	0.95	0.99	0.97	0.88	1.00	0.94	0.97	0.99	1.00	0.96	0.97	0.92	1.00	0.99	0.97	0.99
maxF	1.00	0.99	0.87	0.89	0.99	0.86	0.98	0.99	1.00	0.98	0.98	0.90	0.99	0.99	0.98	0.99
mean freq	-0.99	-0.82	-0.94	0.88	0.90	-0.21	-0.99	-0.93	-0.98	-0.95	-0.98	-0.96	-0.94	-0.86	-0.97	-1.00

748

749

750 **Table 3.** Correlation coefficients between *CISI* and the five force parameters *meanF*, *rmsF*, *rangeF*,

751 *maxF*, and *meanfreq*. The strength of the correlation is coded with a color gradient, highlighting the

752 strong positive (> 0.8) (dense red) and strong negative (< -0.8) (dense blue) correlations.

753

754

755

756

757

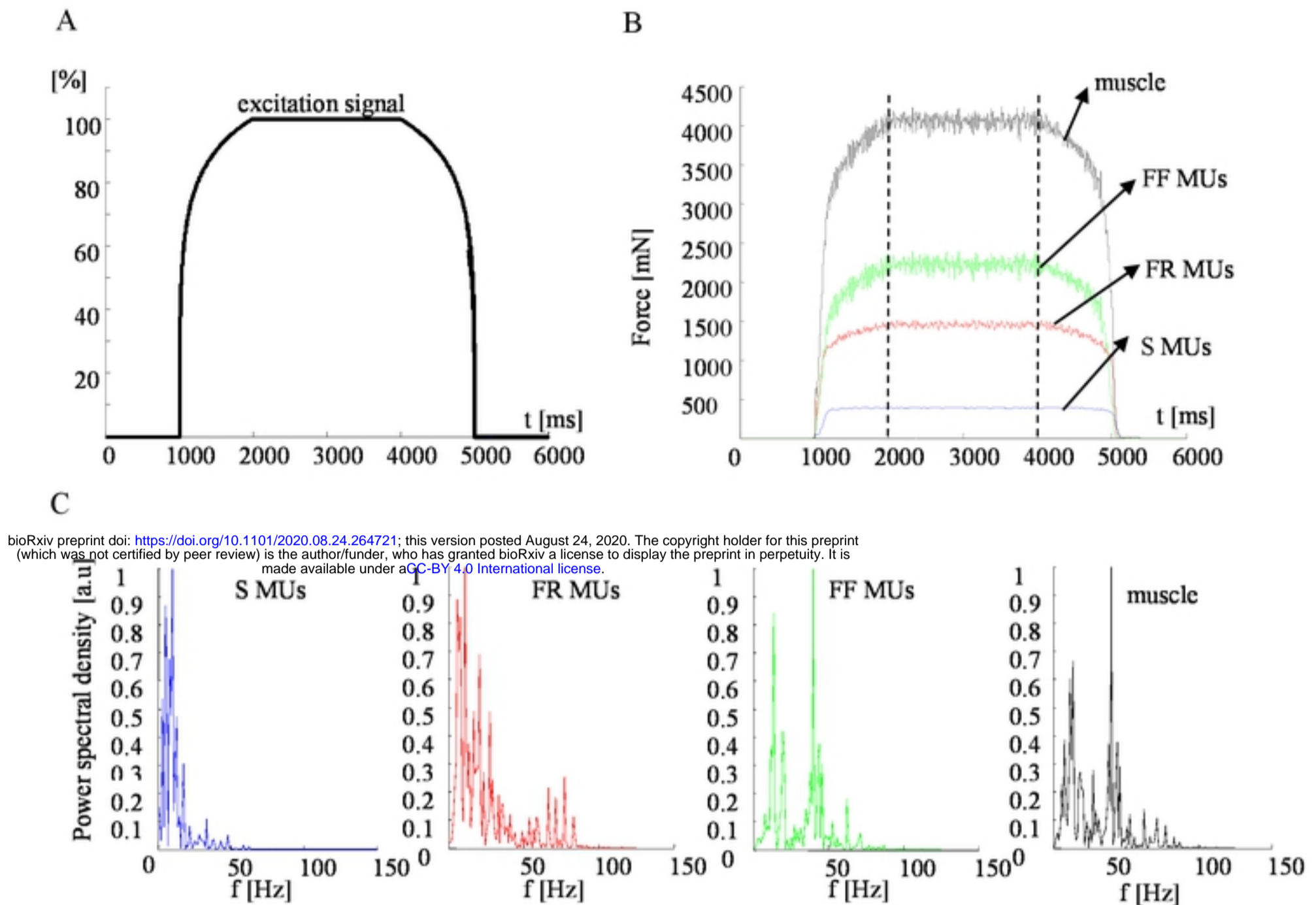


Figure 1. Parameters of the basic model, calculated using a 100% excitation signal. **A.** The law for the excitation. **B.** The calculated forces of populations of different MU types (S, FR, and FF) and the muscle. **C.** Normalized power spectral density of the force during a time period of 2000 to 4000 ms, presented separately for individual MUs (S, FR, and FF) and the whole muscle.

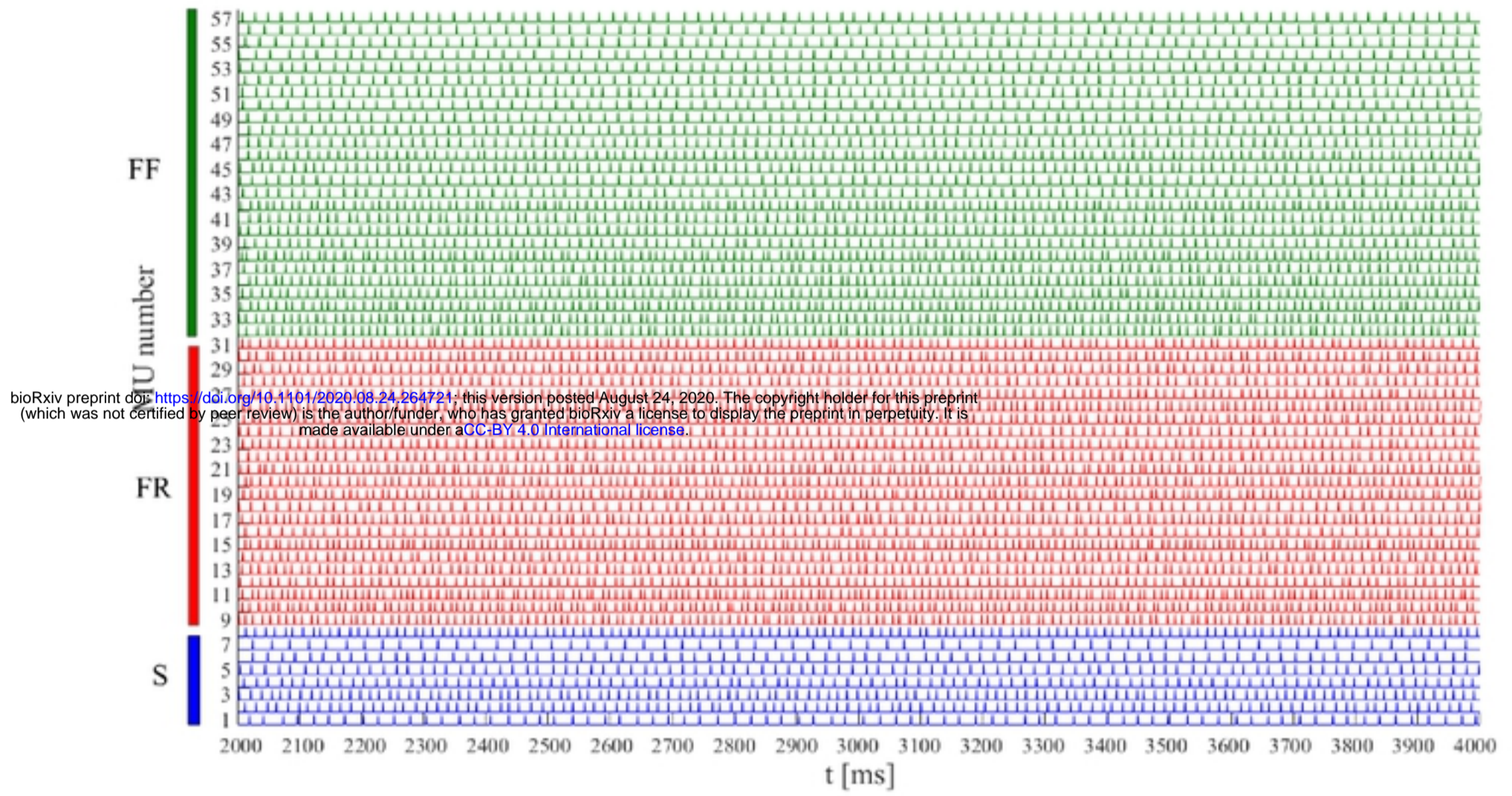


Figure 2. Firing patterns of 57 MU of the basic *NS* model during the time period of 2000 to 4000 ms. MUs are numbered in an ascending order based on their maximum twitch forces within each type: S (1–8), FR (9–31), and FF (32–57).

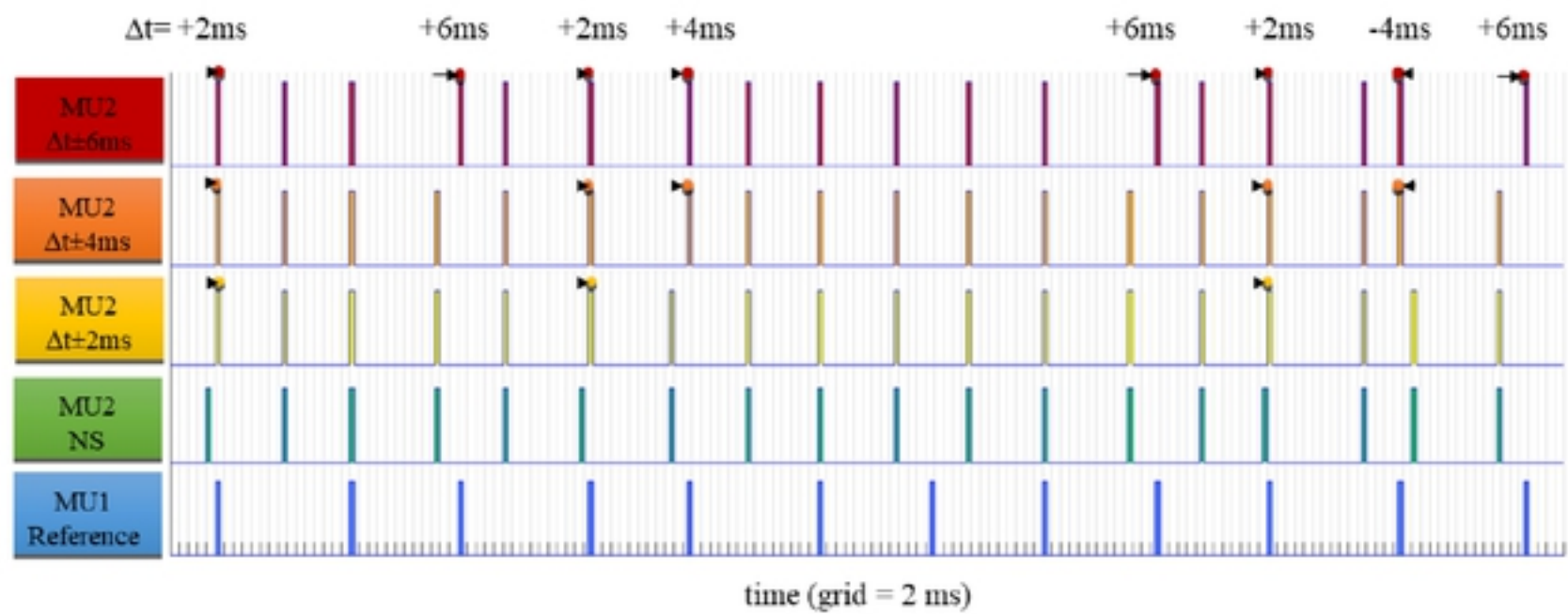


Figure 3. Illustration of the synchronization principle of basic MU firing patterns of two

bioRxiv preprint doi: <https://doi.org/10.1101/2020.08.24.264721>; this version posted August 24, 2020. The copyright holder for this preprint (which was not certified by peer review) is the author/funder, who has granted bioRxiv a license to display the preprint in perpetuity. It is made available under aCC-BY 4.0 International license.

MUs, considering MU1 as a reference one (blue, bottom), and applying the synchronization of pulses to MU2 (green, NS). Three time windows were used: $\Delta t = \pm 2$ ms (yellow), ± 4 ms (orange), and ± 6 ms (red). The dots highlight individual pulses of MU2, which were shifted in time (left or right, as indicated by arrows) to coincide with reference impulses of MU1 when the time interval between the pair of impulses of MU2 and MU1 was less or equal than $|\Delta t|$. The level of synchronization was proportional to Δt , illustrated in this example by increasing numbers n of shifted impulses—namely, $n = 3$ for $\Delta t = \pm 2$ ms, $n = 5$ for $\Delta t = \pm 4$ ms, and $n = 8$ for $\Delta t = \pm 6$ ms.

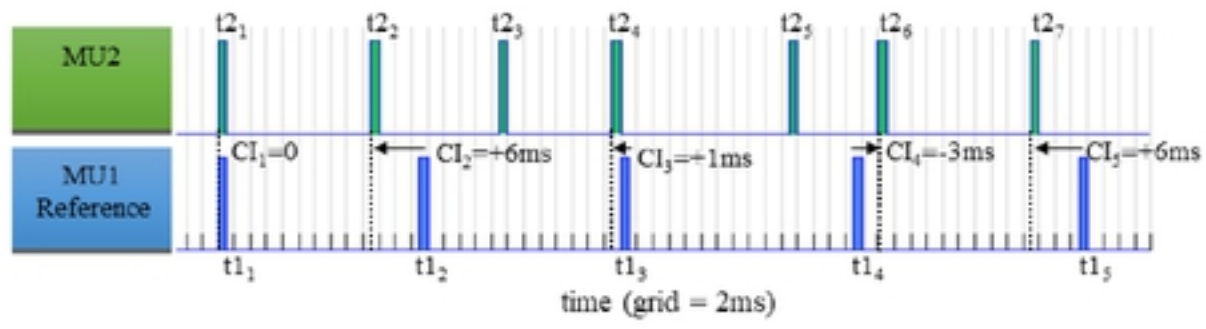


Figure 4. Illustration of the cross-interval measurements of pulses of real MU firing patterns $\{CI_1, CI_2, CI_3, CI_4, CI_5\}$, considering MU1 as a reference (blue, bottom) and applying pairwise differences between the times of occurrences of all MU1 pulses $\{t1_1, t1_2, t1_3, t1_4, t1_5\}$ and their corresponding closest neighboring pulse times of MU2 $\{t2_1, t2_2, t2_4, t2_6, t2_7\}$.

bioRxiv preprint doi: <https://doi.org/10.1101/2020.08.24.264721>; this version posted August 24, 2020. The copyright holder for this preprint (which was not certified by peer review) is the author/funder, who has granted bioRxiv a license to display the preprint in perpetuity. It is made available under aCC-BY 4.0 International license.

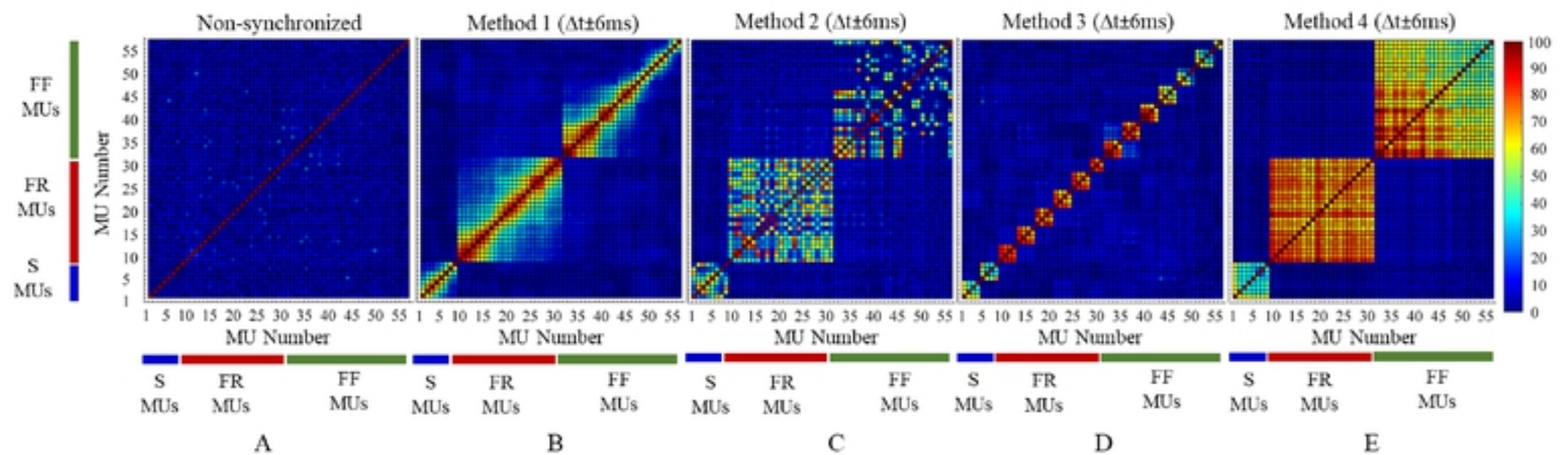


Figure 5. The correlation coefficients ($corMU$) between all pairs of 57 MU firing patterns for the *NS* model and for the four methods of MU synchronization using $\Delta t \pm 6$ ms. The color map represents $corMU$ values in the range of 0% to 100% calculated within the square grid (57×57) of sequential MU numbers from 1 to 57. The diagonal elements of the color map correspond to a 100% correlation between the firing pulses of identical MUs.

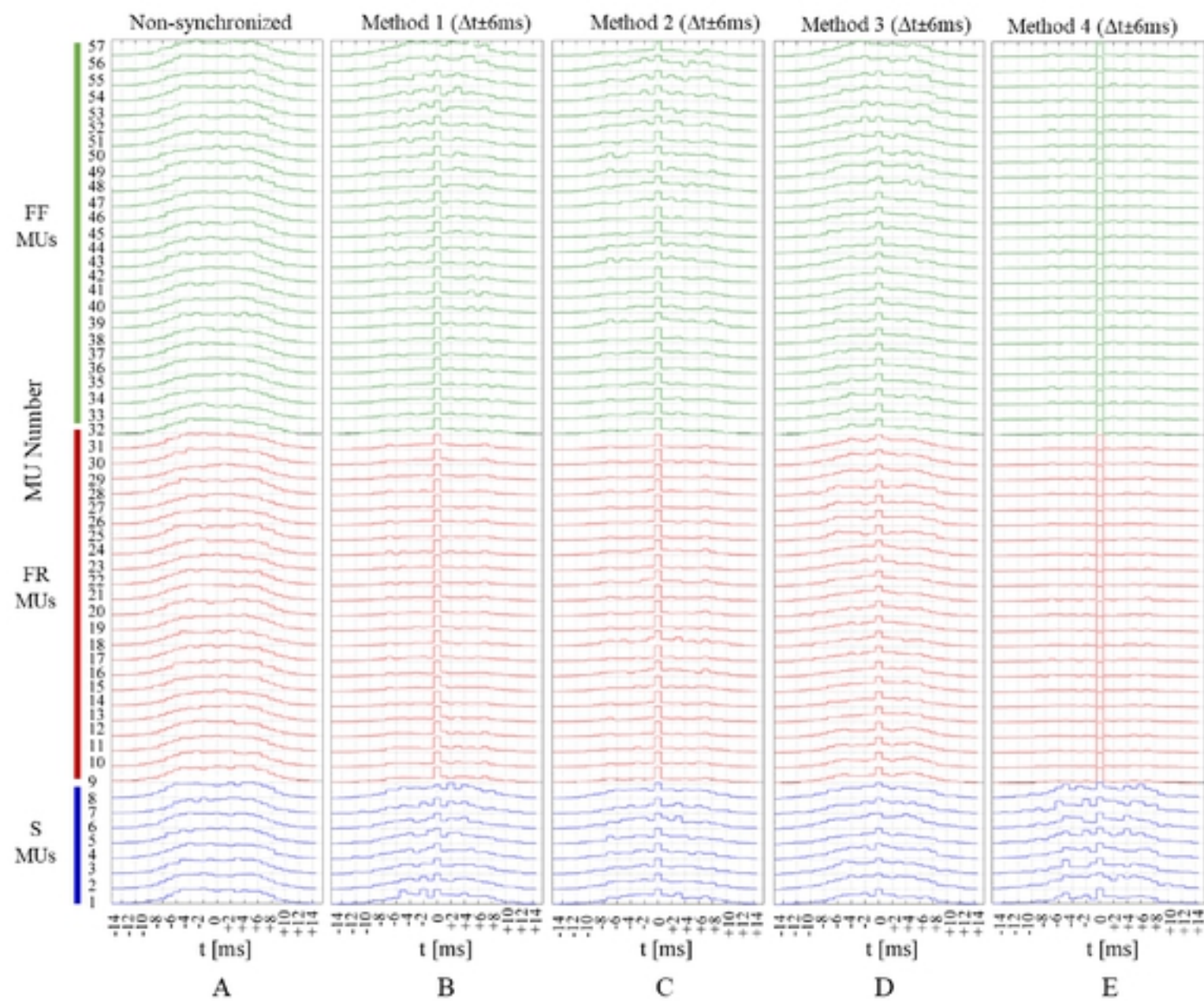


Figure 6. Cross interval histograms of all 57 MU firing patterns for the *NS* basic model and the four methods of MU synchronization using $\Delta t \pm 6$ ms. The cross-interval histograms are depicted with maximal bin normalization, considering a bins width of 1 ms within a bin interval of ± 15 ms. The amplitude of the central bin, presenting a minimal cross-interval difference of ± 0.5 ms, is proportional to the derived index of synchronization (*CISI*).

bioRxiv preprint doi: <https://doi.org/10.1101/2020.08.24.264721>; this version posted August 24, 2020. The copyright holder for this preprint (which was not certified by peer review) is the author/funder, who has granted bioRxiv a license to display the preprint in perpetuity. It is made available under aCC-BY 4.0 International license.

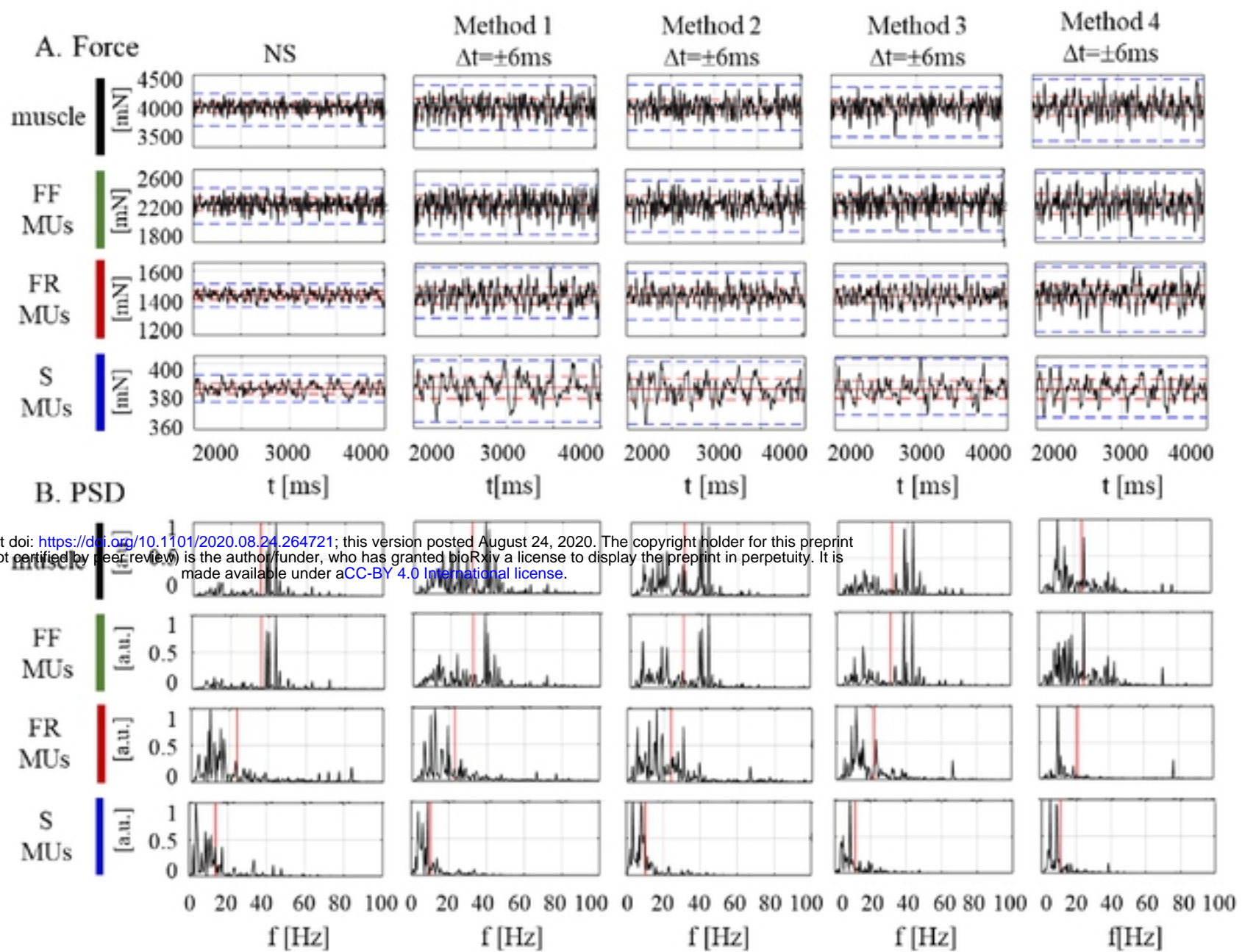


Figure 7. The forces (A) and respective power spectral densities (B) calculated for the muscle and different MU types (S, FR, and FF) during the muscle steady state of the *NS* excitation and by using four methods of MU synchronization ($\Delta t \pm 6$ ms). Values of different force parameters are indicated in each box of panel A as follows: the mean force by a red horizontal solid line, the force *rms* by a red horizontal dotted line, and the force range by a blue horizontal dotted line; meanwhile, the mean frequency is indicated in each box of panel B by a red vertical tick line.

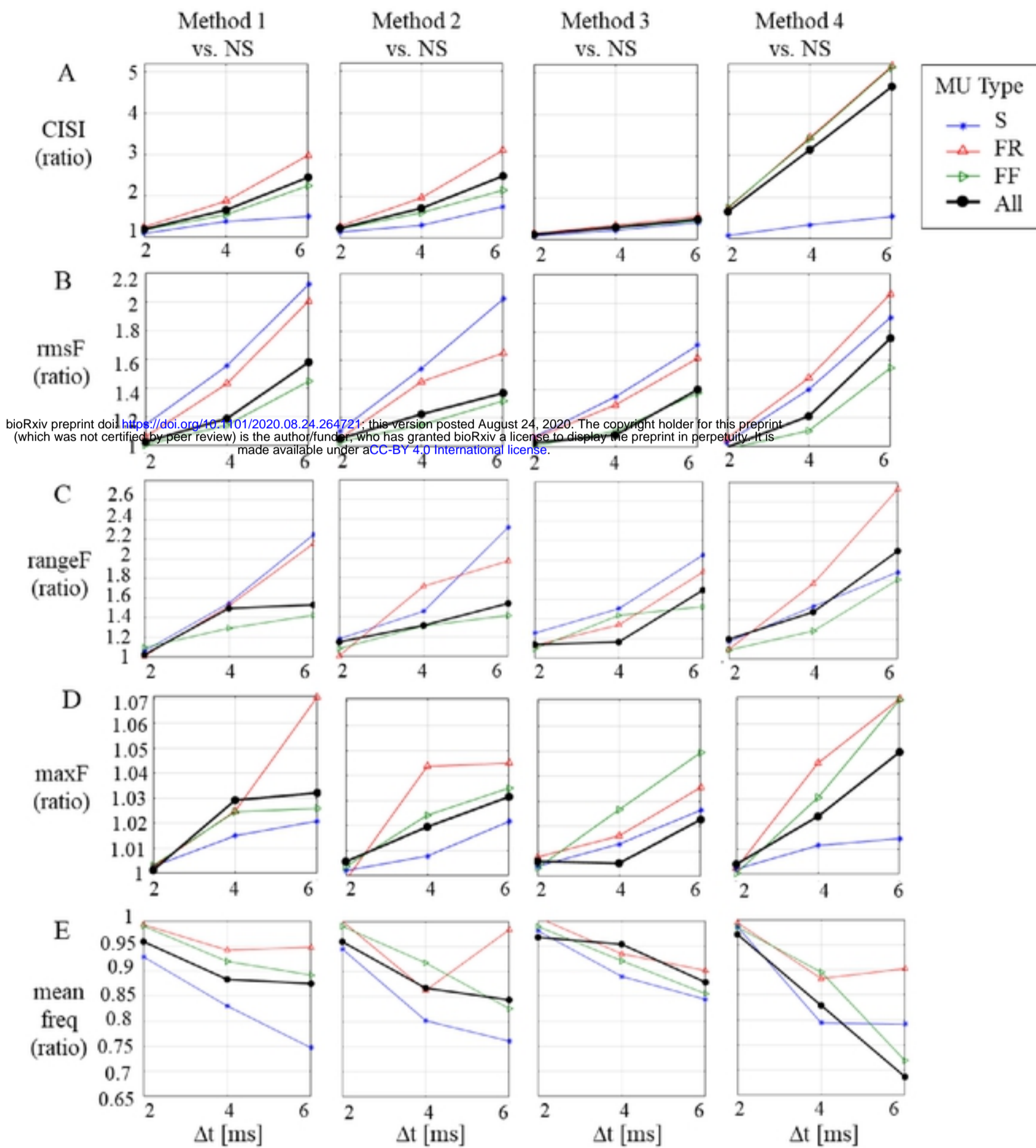


Figure 8. Effects of widening the time window for synchronization ($\Delta t = \pm 2, \pm 4,$ and ± 6 ms) on an increment of the cross-interval synchronization index of MU pulses (CISI in panel A), the force *rms* (panel B), the force range (panel C), the maximal force (panel D), and the force mean spectral frequency (panel E), presented as the ratio of values calculated for each method of synchronization (Methods 1–4) vs. the *NS* model.